Ročník 2022 electroscope Číslo I

# Automated defectoscopy of thin poly (methyl methacrylate) layers

J. Podstránský, A. Knápek
*Institute of Scientific Instruments of the CAS, v. v. i.,*
*Královopolská 147, 612 64 Brno, Czech Republic*
podstransky@isibrno.cz

## Abstract

In the electron beam lithography process, one of the initial steps is to coat the substrate (i.e., the silicon wafer) with a thin layer of polymer resist. During the coating process, defects in the thin layer can occur, which can affect the exposure and therefore the functionality of the final nanostructure. By checking the quality of the deposited polymer layer prior to exposure, these defect sites can be avoided. This process can be done manually using a visible-light microscope, but it is a time-consuming process and subject to a possible human error. In the framework of this project, a fully automated device has been developed that can detect and identifies these using computer vision. It is a scanning device that, by combining three stepper motors and an optical camera, takes images of the desired area of the wafer and then analyses these with the help of artificial intelligence. The user is then provided with a document in which the size, position and type of each defect found is recorded.

**Keywords:** defects in resist, artificial intelligence, image processing, automatization

## 1. Introduction

Electron beam lithography (EBL) is one of main methods used for nanofabrication, for patterning mesoscopic structures or systems with unique advantages of high resolution, yielding high accuracy in positioning, high reliability in processing, and high flexibility in patterning replication. This process is most often done on a silicon wafer. Nowadays, resolution capability is as good as sub 10 nm [1]. The whole process consists of multiple steps. The focus is on resist layer deposition and its perfection. It is one of the initial steps, and the most crucial one to get the desired pattern. In our laboratories, this step is most often executed by the means of spin-coating. During the deposition of resist by spin-coating, various defects can occur: starting from dust contamination, micro-bubbles, bumps, craters, to comets and thickness inhomogeneity [2][3].

Until now, the process of defect detection in the resist is done manually under a visible-light microscope. In our laboratory, a scientist has so far measured it manually in rows of 3 mm wide, in an area of about 50 × 50 mm. Every defect that is found is measured, given coordinates and written in a chart. Due to the preciseness and the scale of this work, every wafer takes a dozen of minutes to be inspected. In addition, the combination of a loose wafer and the possibility of human error can lead to reduced measurement accuracy. To improve the defectoscopy process, the WaferScan instrument presented below was developed to semi-automate the process of scanning thin polymer layers and analyzing defects using computer vision.

### *1.1 Defects in the electron resist*

Any parts of the film where the homogeneity of the layer is disturbed are called defects. These disturbances make the area unpredictable, which leads to faulty results. Defects that can occur during the resist layer preparation can be divided in two groups. The first group is caused by impurities that land on the resist layer, such as dust particles and fibers. Particles and fibers can be reduced, which reduces the defects, by using a laminar flow box that filters the air that surrounds the specimen or lowers the number of particles in a whole. Air cleanliness in clean rooms is classified by the International Organization for Standardization (ISO) [4]. Another way for particles to get to the specimen is through the impurity of the substrate or resist. In practice, to get rid of these impurities, dust-free gases are used, as $N_2$. With a help of a blow gun, the surface of a substrate is cleaned immediately before deposition of the resist. Another technique used utilizes ultra-filters that are installed on the injection, before the deposition of the resist solution.

If any impurity falls on the surface of the wafer during spin coating, it makes a thickness difference in the resist that is being distributed from the center to the edge of the wafer. This defect is visible as a "comet" shape as can be seen in Fig. 1a. Other impurities are small resist flakes that stick to the layer and get permanently attached to the surface due to the baking (Fig. 1b).

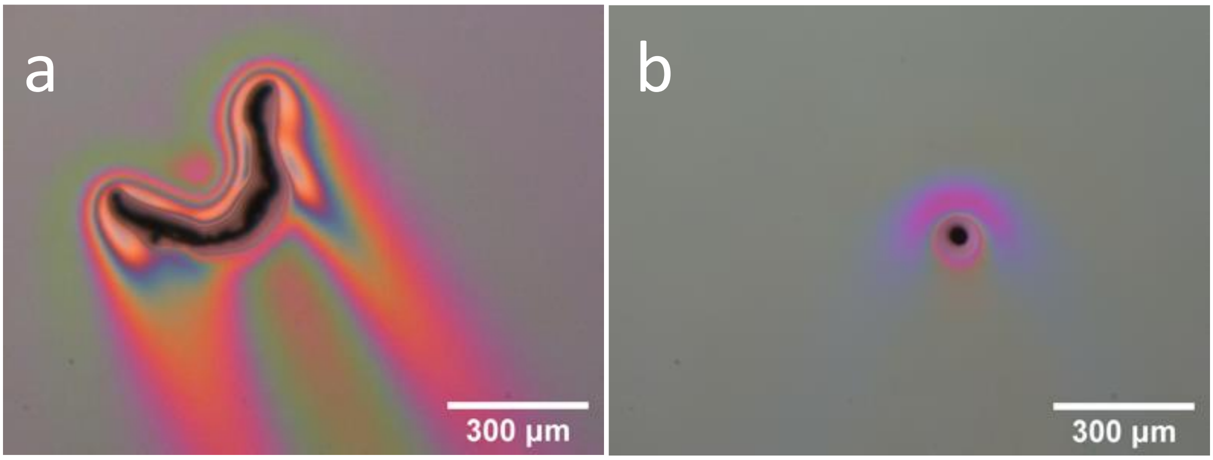

Fig. 1: The two types of common defects that can be found by WaferScan system: (a) A defect caused by a fiber, (b) A defect caused by a resist flake.

The other group of defects is caused by errors in the processing technology. Defects that occur during the spin coating procedure are generally observed radially. One of the defects that can be detected is due to bubbles in the resist mixture. This defect can take place in the resist if air bubbles are incorporated by moving the resist in whatever manner, e.g., pipetting, transporting, shaking, etc. Defects caused by these bubbles make small spots in the resist layer with a thickness difference, which causes problems during the exposure, such as cracks in the resist layer around these spots. These defects are shown in Fig. 2b [5]. The chance of this happening can be lowered by slowly pouring and ultra-filtering the resist while pipetting it, degassing the mixture in a desiccator, and reducing the movement of the resist container.

Two more defects can arise. One of them is represented by spots that are not covered by any resist. This happens if an insufficient amount of resist is applied. Spots will appear on the edges of the substrate due to the principle of the already mentioned spin coating process. The other of the two is caused due to an insufficient centering of the wafer on the spin coater.

Microscopes are not able to see this defect that easily due to a small field of view. As can be observed from Fig. 2a, this defect is more easily observed at the macroscopic scale, by the naked eye or optical instruments which have a larger field of view than a microscope [6].

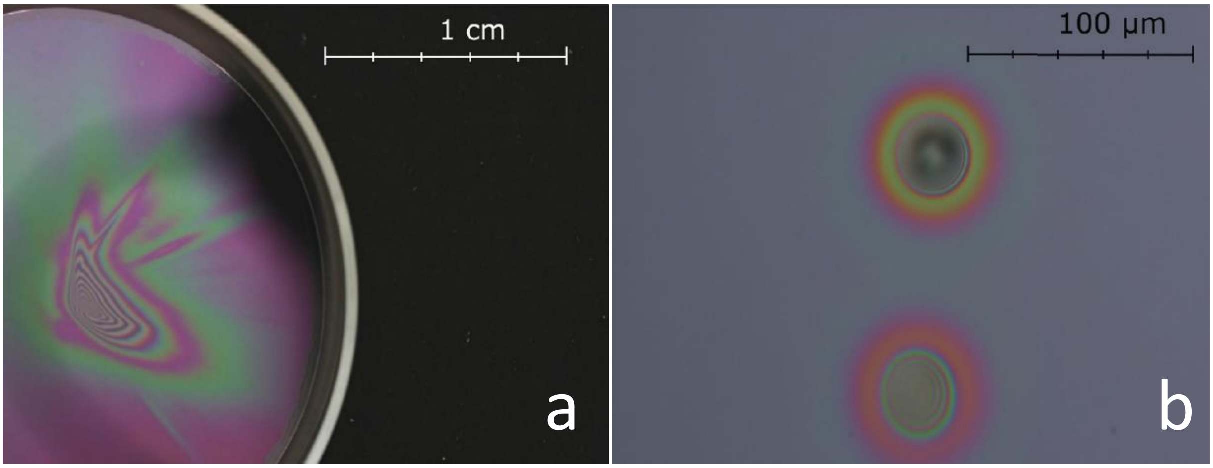

Fig. 2: Two types of faults that WaferScan is unable to find: (a) A wafer with an inhomogeneous layer, (b) A defect caused by micro bubbles.

## 2. Measurements and results

In order to achieve a system capable of displaying the described defects, the concept of the WaferScan system, as shown in Fig. 3, was developed, and computer vision-based software was developed along with it. The system is designed to take images of the wafer in a user-selected zone by moving the wafer, and then process the acquired images to find all captured defects. The process of completing the entire system is described in the following two sections, 2.1 and 2.2.

Fig. 3: Mechanical design of the WaferScan system, the final frame concept based on aluminum profiles and industrial stepper motors.

### *2.1 Hardware design*

Fig. 4 shows the main electrical components of the system. Both already mentioned stepper motors share the power supply that provides 36 VDC. Axes are equipped on each end with an inductive proximity sensor. These sensors activate when the holder of a wafer gets nearby. If sensors activate, the power to the corresponding axis stepper motor is turned off to prevent any further damage that could occur. Another electronic component around which more electronics are placed is the LED ring, which consists of 16 diodes. The ring is connected to the Arduino UNO which can work as a communication canal and a power supply. In the system setup, Arduino works only as a communication canal due to its limitations. Arduino is also able to provide only 500 mA which is not enough to achieve the maximum illumination that the LED ring is capable of. For maximum capabilities, 800 mA from the external power source is provided. The camera's power drain is only 4.4 W. Such a demand is fully covered by a power supply embedded within the USB 3.0 interface.

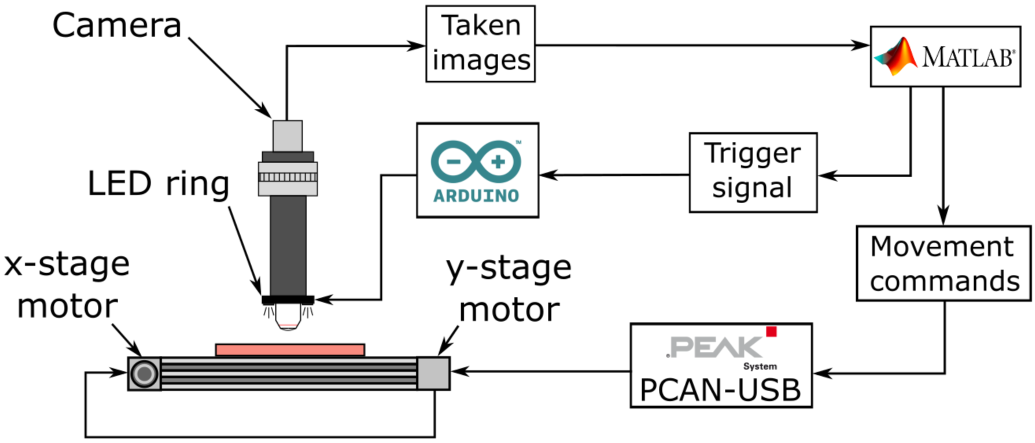

Fig. 4: Block diagram showing electronic components and main communication channels of the WaferScan.

## 3. Algorithmizing

This section describes the options of the system that are provided to the user and gives the reader a step-by-step understanding of how the Main function that looks for the defects on the wafer works and what data the user gets from performing it. In Fig. 5, it can be seen that the process is divided into three steps, "Initial Process", "Scanning Process", and "Image Processing".

In "Initial Process" a program does a calibration of the system and all necessary calculations to start a precise measurement [7]. The target of the following "Scanning process" is to take images of a whole user-desired area. During the last process that is called "Image Processing", images are post-processed to get the needed data from them. Users have the option to choose from two options. The first option is to not create the image and continue with analyzing the image for the defects. The second option is to create the stitched image and continue with the first option. The third option gives the user the ability to create only the stitched image. This function is used mostly for testing. It allows the user to examine the samples that already have some fully developed patterns.

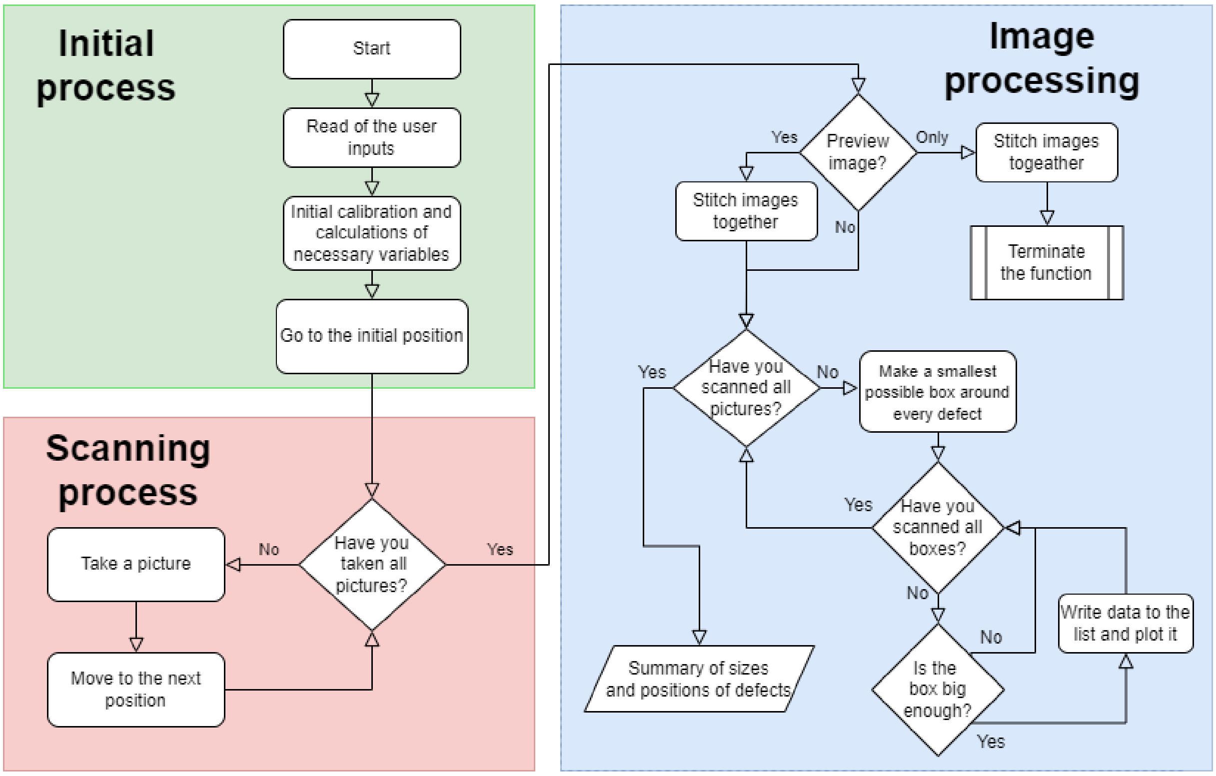

Fig. 5: Flowchart describing the implemented algorithm.

This is followed by an analysis of the image in which defects are sought. The whole process is done in cycles by loading and evaluating the images one by one. The images that are captured by the system do not contain much noise or parasitic light. As a result, there is no need for the image to undergo its removal where the size of the defects could then be distorted. The only image modification that the system does is the conversion from a grayscale image to a binary image. This is achieved by thresholding.

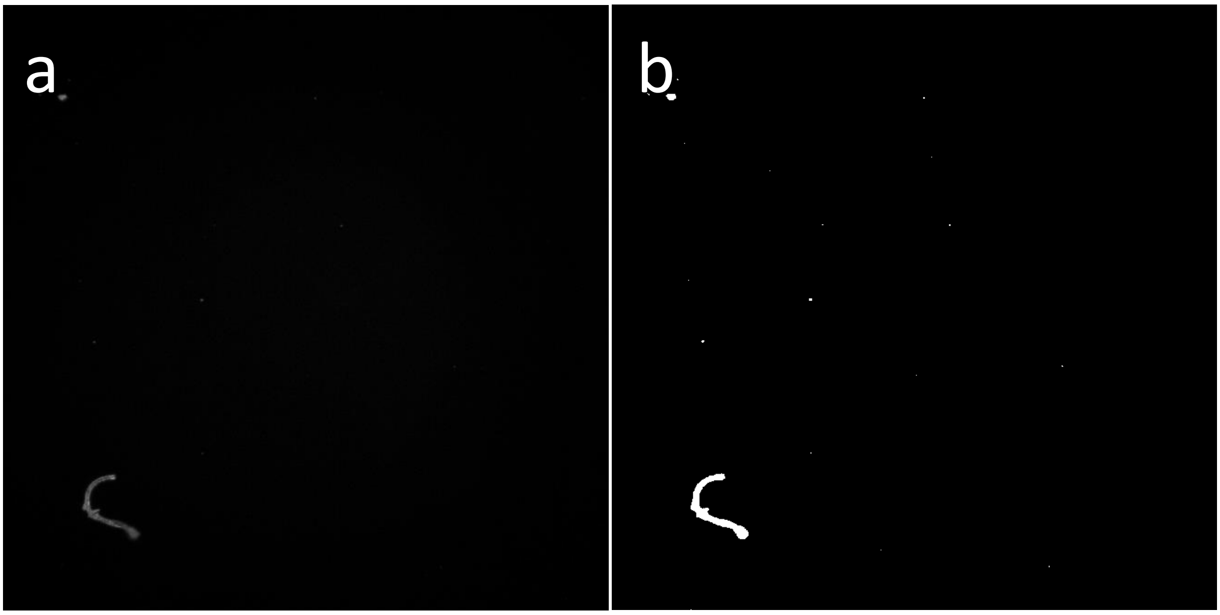

Fig. 6: The image before and after the thresholding: (a) Unmodified image, (b) image modified by thresholding.

In the system, the thresholding is a constant $t$. The process is defined by the following equation, where $x$ represents the pixel value in the grayscale image (Fig. 6). The thresholding value is set to be constantly 20. For $x \geq t \Rightarrow$ the new pixel is equal to 1; for $x < t \Rightarrow$ the new pixel is equal to 0. After this conversion, the pixels corresponding to value 1 are taken as defects, and pixels with value 0 are taken as a background.

The next step is to measure the properties of defects in the image. For this purpose, a *region props function* contained within Matlab Image Processing Toolbox was used, with a property "Bounding Box". It looks for the smallest box containing the whole defect. It then returns the coordinates of the upper-left corner of the box and the lengths of its sides. If a dimensions of the field of view and the image resolution are known, the obvious step is to convert the measured values in pixels to micrometers. The system then goes through the list of boxes that now represent the defects. If any of the sides of the box are larger than the value specified by the user, this defect is written to the final list of found defects and further examined by artificial intelligence to determine whether it is dust or fiber. Results can be seen at Fig. 7 [8].

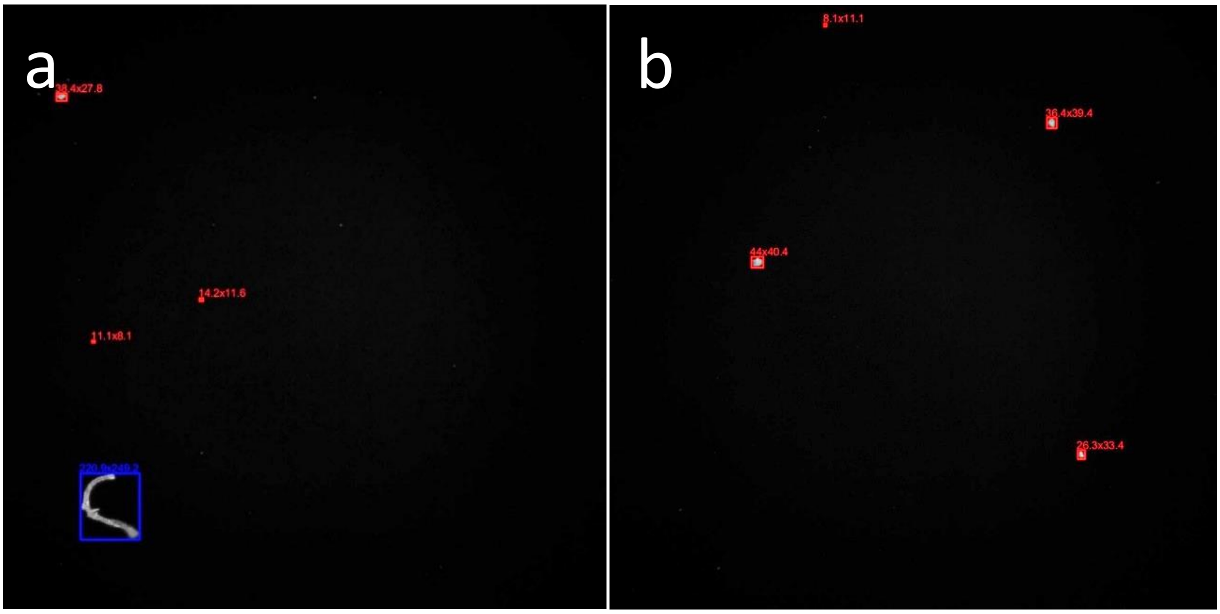

Fig. 7: Measurement of the size, position, and type of the defects; red boxes surround dust particles and blue boxes surround fibers: (a) An image with a fiber and dust particles, (b) An image only with dust particles.

## 4. Conclusions

The aim of this measurement was to compare the accuracy of the currently used manual method with the constructed system. In addition, it was a test of how long it would take the system to analyze a 50 × 50 mm area for 10µm defects. Both measurements were performed in a flow box. The wafer number 1 was set to be analyzed first by the human operator. His analysis took around 1 hour and was able to find 9 defects in the predefined area. The outcome data set is shown in Fig. 8a. Immediately after that, the analysis by the WaferScan system took place. The full procedure took 27 mins and found 33 defects. The outcome data set is shown in Fig. 8b.

The second wafer was prepared for testing first by WaferScan and then by manual method. The software found about 60 defects and took 50 mins. The analysis took so long due to the lack of RAM. Manual analysis was not carried out because of the number of faults that were found by the AI. The manual method would take around two hours with this number of defects. The conclusion of this experiment is as follows. The system has the potential to achieve greater defect measurement accuracy than the current manual method.

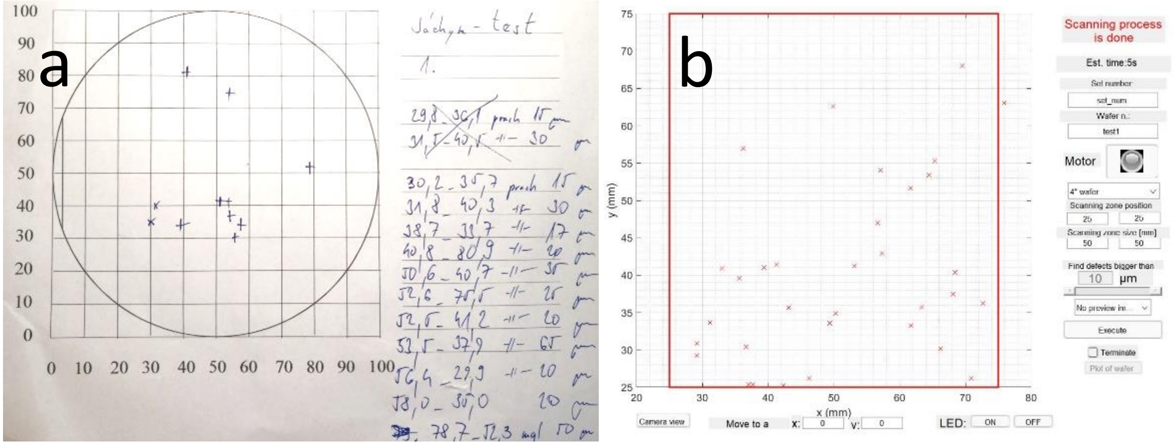

Jáchym - test

1.

~~29,8 – 30,1 prach 15 μm~~
~~31,5 – 40,5 -||- 30 μm~~

30,2 – 35,7 prach 15 μm
31,8 – 40,3 -||- 30 μm
38,7 – 33,7 -||- 17 μm
40,8 – 80,9 -||- 20 μm
50,6 – 40,7 -||- 35 μm
52,6 – 75,5 -||- 25 μm
52,5 – 41,2 -||- 20 μm
53,5 – 37,9 -||- 65 μm
56,4 – 29,9 -||- 20 μm
58,0 – 30,0 20 μm
78,7 – 52,3 mgl 50 μm

Scanning process is done
Est. time:5s
Set number: set_num
Wafer n.: test1
4" wafer
Scanning zone position: 25 25
Scanning zone size [mm]: 50 50
Find defects bigger than 10 μm
No preview im...
☐ Terminate

Fig. 8: Results of the comparing measurement: (a) Manually analyzed data set; (b) Data set analyzed by WaferScan

The aim of this work was to create a system capable of detecting defects in thin polymer layers fully automatically. This development included both hardware and software solutions to the problem. To conclude, a device was developed that allows defects larger than 7 µm to be monitored. The cost of manufacturing it is millions of kroner cheaper than commercially available devices for detecting defects in resists.

## References

[1] HU, W., et al. Sub-10 nm electron beam lithography using cold development of poly (methylmethacrylate). *Journal of Vacuum Science & Technology B: Microelectronics and Nanometer Structures Processing, Measurement, and Phenomena*, 2004, 22.4: 1711-1716.

[2] KNÁPEK, A., et al. Automated System for Optical Inspection of Defects in Resist-coated Non-patterned Wafer*. Jordan Journal of Physics*, 2020, 13.2: 93-100.

[3] DROZD, M. *Návrh automatizované aparatury určené pro inspekci křemíkových desek ovrstvených PMMA [online]*. Brno, 2020 [cit. 2022-03-19]. Accessible from: https://www.vutbr.cz/studenti/zav-prace/detail/140771.

[4] WHYTE, W. *Cleanroom technology: fundamentals of design, testing and operation*. John Wiley & Sons, 2010.

[5] KOCH, C. and RINKE, T. *Journal of Photolithography: Basics of Microstructuring. MicroChemicals GmbH*, 2017.

[6] Magnification and resolution, Science Learning Hub, The University of Waikato [online], [cit. 2022-04-02]. Accessible from: http://www.sciencelearn.org.nz/Contexts/Exploring-with-Microscopes/Science- Ideas-and-Concepts/Magnification-and-resolution

[7] Controller Area Network (CAN) Overview, National Instruments Corp. [online, 2022-04-21]. From: https://www.ni.com/cs-cz/innovations/whitepapers/06/controller-area-network–can–overview.html

[8] Corr: 2D correlation coefficient, The MathWorks, Inc., [online], [cit. 2022-05-14]. Available from: https://www.mathworks.com/help/images/ref/corr2.html